A New Insight of Talang Akar Formation in the Ridho Field, North Palembang Sub-basin, Indonesia: An Integrated Approach

Togi Y. Sitinjak[1#], Ricky A. Tampubolon[1], Ardian Pratama[1], Wildanto P. Nusantara[1], Aziza Muis[1] and Harsanti Setiani[2]

[1]Subsurface, Odira Energy Karang Agung Ltd, Jakarta, Indonesia
[2]PT. Geoservices Indonesia, Jakarta, Indonesia
[#]Corresponding author: togi.y@odiraka.co.id

ABSTRACT

The synrift sandstone deposits of Eo-Oligocene Lemat (LMF) and Oligo-Miocene Talang Akar Formations (TAF) are the most well-known hydrocarbon reservoirs in the South Sumatra Basin, Indonesia. However, only limited studies on TAF in the North Palembang Sub-Basin have been published. In the Ridho field, TAF is characterized by fining-up sequences of inter bedded, fine to medium-grained sandstones and shales overlain by a coal layer as the top marker, while LMF comprises of continuous blocky-shaped, medium to coarse-grained, conglomeratic sandstones.

Previous lithostratigraphy-driven sand to sand correlation between wells has created difficulties in understanding the geology and in producing consistent correlation, especially within the TAF. In order to define chronostratigraphy-based correlation and interpret the depositional environment of TAF and LMF, an integration between palynological, core study and petrophysical analysis was performed. The result of this integrated approach demonstrates aligned hypotheses. The occurrence of pollen Meyeripollis naharkotensis and Florschuetzia trilobata along the studied wells suggest Late Oligocene age. The palynology study subdivides TAF into three backmangrove-intertidal sand units with an increase of marine influence defining a transgression to the top of the TAF. The transgressive event is identified in core sample by lesser tidal influx sedimentary structures such as ripple, mudlayer, flaser and also finer grained sandstone at the top of TAF. Furthermore, based on petrophysical evaluation, better sand quality with lower NTG (net-to-gross) near top TAF confirms the retrogradational event in this formation.

The new sand unit definitions from the current study provide more consistent correlation in terms of sand thickness and characteristics for future modeling purposes.

Keywords: Talang Akar Formation, North Palembang Sub-Basin, South Sumatra Basin

INTRODUCTION

Background

The South Sumatra Basin is located on the southern part of Sumatra Island. It is bounded from Central Sumatra Basin to the north by Bukit Tiga Puluh Mountain and from Sunda Basin to the south by Lampung High. South Sumatra Basin consists of four sub-basins, namely: Jambi, Central Palembang, North Palembang, and South Palembang Sub-basins (Figure 1).

Ridho field in the North Palembang Sub-basin was discovered in 2009. Since its discovery, Talang Akar and Lemat Formations have been the main producing zones with a total production of approximately 160 MBOE from three wells. In total, six wells have been drilled in the Ridho structure, with four of them being active producers, while the rest are water injectors. Recent development activities of the field are currently progressing in order to enhance production and find more upside potentials. One of these development activities is updating the reservoir model that was previously done under the POD project in 2009. The updated reservoir model will later be used as the basis to propose drilling additional development wells.

The POD version of Ridho field's reservoir model utilized geological data that were acquired from the first two wells in the field, which consist of R-1 and

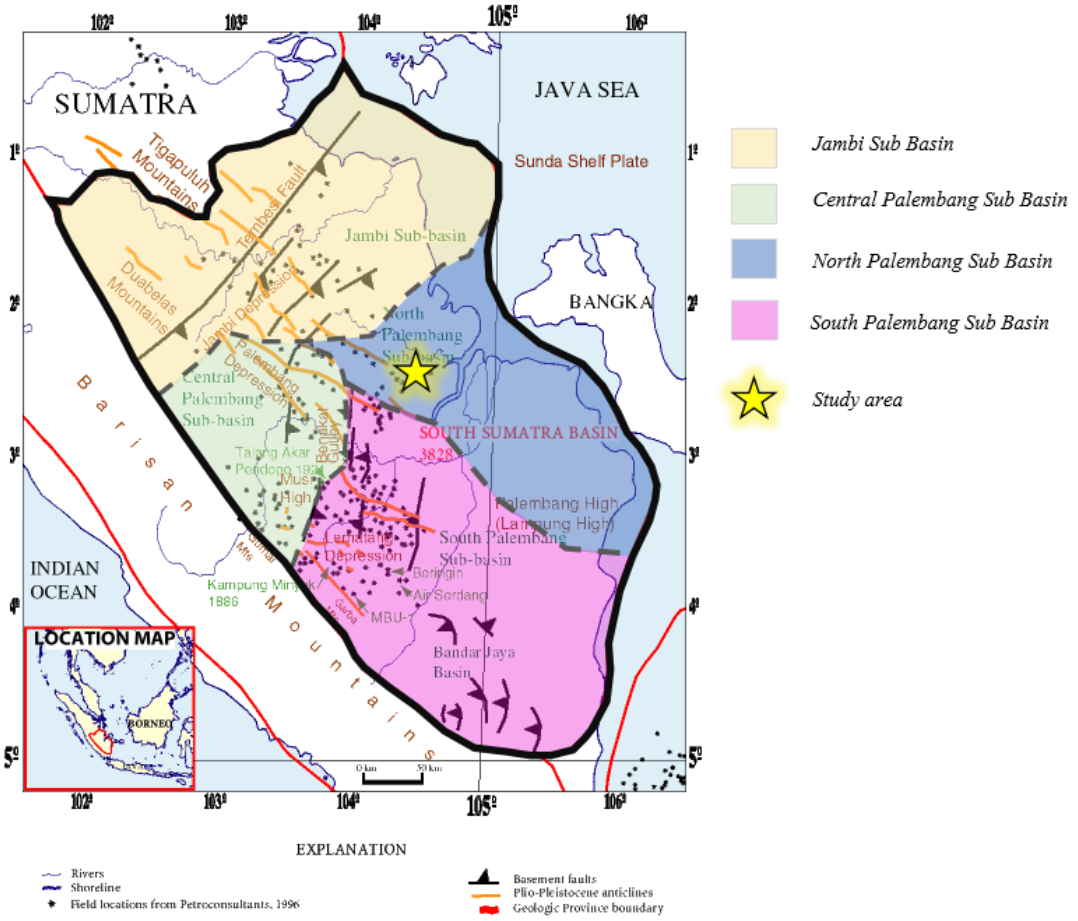


Figure 1: *Index map of the South Sumatra Basin Province, showing major structural features. The structures were assembled from Hutchinson (1996); Williams et al. (1995); Moulds (1989); van Bemmelen (1949) [after Bishop, 2001]. Highlighted yellow star is location of the current study.*

R-6. The data includes well correlation, petrophysical evaluation, and facies modeling. The more recently updated reservoir model incorporates data from four new development wells. These data consist of wireline logs, cores, and lab analyses such as palynology, RCA (Routine Core Analysis) and SCAL (Special Core Analysis).

One of the primary inputs to reservoir modeling is facies modeling based on sand to sand correlation between wells. Previous facies model (the POD version) was built by employing lithostratigraphy-based sand correlation. This lithostratigraphy technique correlates sand to sand in each well based on similarities in wireline log characters (e.g. Gamma Ray-GR, Resistivity, Density-RHOB and Neutron-NPHI logs) and also similarities in lithology composition from cuttings and core description. This technique sometimes can lead to confusion or mis-interpretation. For instance, a look-a-like sand across the wells is later proven disconnected pressure-wise, or in other words, it is not the same sand body as expected from the initial correlation. Another disadvantage of lithostratigraphy correlation is that it doesn't show the effect of geological evolution such as sea level change to the sedimentary process and reservoir quality (Nichols, 2009), which is very critical to consider when making a comprehensive reservoir model. OEKA's internal subsurface team then initiated the current study, which integrates palynological, petrophysical and core analysis data to create a chronostratigraphic sand to sand correlation and obtain deeper geological understanding on Talang Akar and Lemat Formations.

GEOLOGICAL SETTING & SEDIMENTATION HISTORY

South Sumatra Basin has undergone three major tectonic events (Suhendan, 1984), which consist of:

1. Extension during late Paleocene to early Miocene forming north-trending grabens that were filled with Eocene to early Miocene deposits (40-29 Ma);

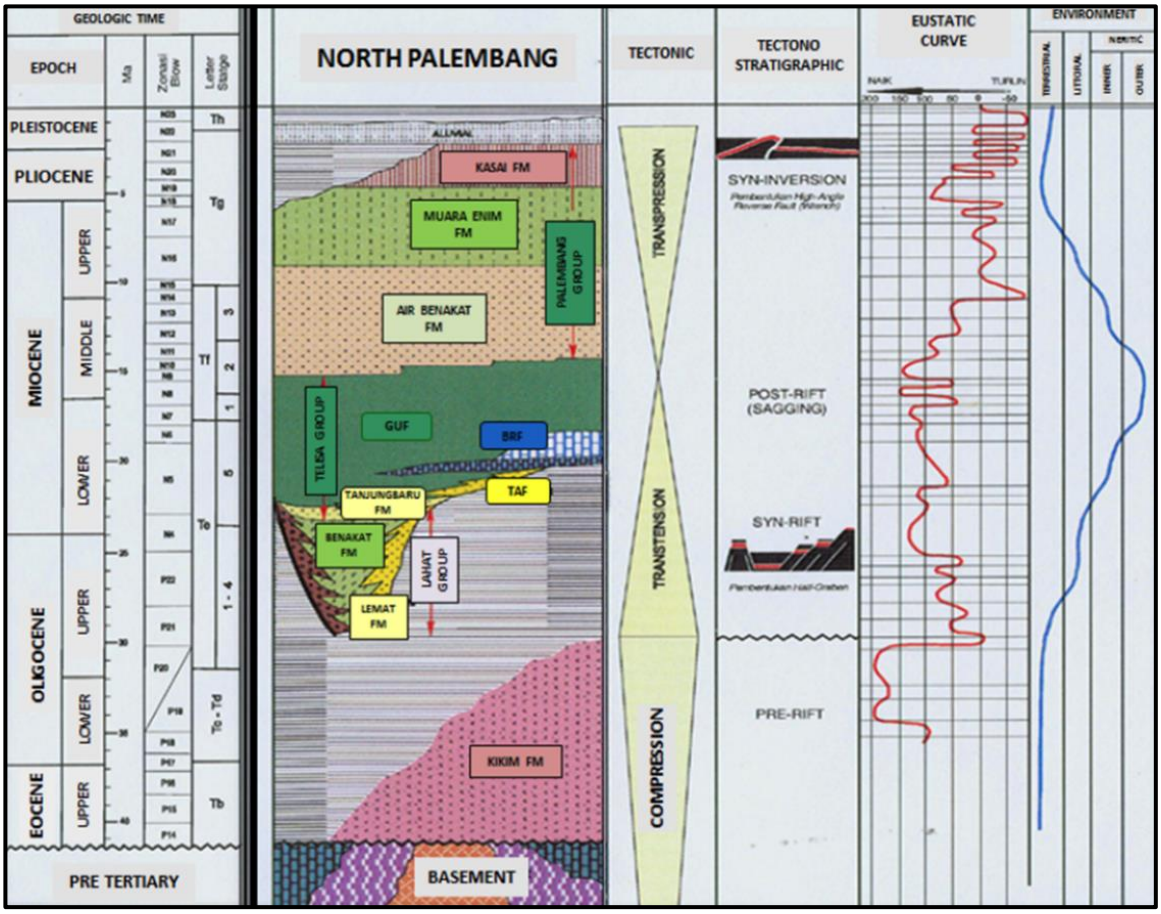


***Figure 2**: Stratigraphic column of North Palembang Sub-basin, South Sumatra Basin. (modified from Syaifudin et al., 2015)*

2. Relative quiescence with late normal faulting from early Miocene to early Pliocene (29-5 Ma); and
3. Basement-involved compression, basin inversion, and reversal of normal faults in the Pliocene to Recent forming the anticlines (5 Ma-Recent) that form major traps in the area.

Sedimentation history in the South Sumatra basin began with the deposition of continental sediments derived from local erosion of Lemat Formation in the Eocene (Cole and Crittenden, 1997; Courteney et al., 1990). As the rifting phase weakened during late Oligocene time, transgression occurred as a result of thermal sag and eustatic gain (Netherwood, 2000; Barber et al., 2005). This transgression event was then followed by sedimentation of Talang Akar Formation in several rifted grabens. The sediments of Talang Akar Formation were deposited in various depositional settings, from fluvial to deltaic and drives mixed sediment strata consisting of interbedded sandstones, shales, and coals. In the earliest Miocene, as the transgression continued, the depositional settings of Talang Akar Formation changed gradually from fluvial to more deltaic and then marginally-deep marine.

During the Early Miocene, deposition of Baturaja Formation flourished on structural highs as carbonate buildups on some local inter-graben highs and basin margins or as carbonate mud-dominated in the low energy banks (Situmeang et al.,1992; Longman et al., 1992). In the deeper part of the basin, a shale-dominated strata with thinly bedded sandstone and limestone intercalation, Gumai Formation, was deposited. During the Middle Miocene's maximum transgression, the Gumai shale seal across the region creating the most widespread regional seal (De Coster, 1974).

In the Middle Miocene, development of the Barisan Mountains and possible volcanic islands to the south and southeast, further decreased and then cut off and overwhelmed marine influences and added new clastic and volcaniclastic sources from those directions (De Coster, 1974; Cole and Crittenden, 1997; Hamilton, 1979).

Deposition during the Middle Miocene-Pliocene compressional regimes started with shallow marine

– deltaic Air Benakat and Muara Enim Formations. Air Benakat Formation consists mainly of sandstone and fine-grained siliciclastic rocks, while coal bed intercalations occur in the Muara Enim Formation.

In the Pliocene, the sedimentation was driven mainly from the west and northwest of the basin which marked the Kasai Formation deposition. This formation overlies the Muara Enim Formation unconformably and consists of conglomerates, tuffaceous sandstone, and tuffs with lignite and silicified wood.

METHODS

This study integrates palynological, petrophysical and core interpretation. Palynological analysis was performed on fifty-four (54) ditch cutting samples from five (5) Ridho wells. These samples picks were based on high Gamma Ray readings. The sample list for palynological analysis is shown in Table 1.

These samples were then utilized for palynological slide preparation. The slides were examined under the microscope for palynological content. Quantitative palynology analyses were carried out for this study. One palynological slide was examined in detail and the palynomorphs were counted. The actual number of specimens of rarer species was counted on the slide and was recorded. Where yields were lean, the total number of specimens on the slide was provided. Fungal palynomorph counts were recorded, but these are complimentary to the standard counts.

In addition to the palynomorphs counts, a visual estimate of the relative proportions of the palynomacerals and structureless organic matter (SOM) was made from the kerogen slide. The identification of these kerogen components broadly follows techniques described by Van der Zwan (1990) and Whitaker et al. (1992). The palynological classification applied is summarized and the main palynomaceral types are described in more details.

Table 1. *Palynological analysis samples of Ridho field.*

Well	Palynology			Samples depth (mMD)
	Ditch Cuttings (#samples)	Sidewall Cores (#samples)	Core (#samples)	
R-1	13	0	0	1318-1320; 1322 – 1324; 1332-1334; 1338-1340; 1346-1348; 1356 – 1358; 1358-1360; 1370-1372; 1372-1374; 1380-1382; 1440-1442; 1442-1444; 1452-1454
R-2	11	0	0	1324-1326; 1338-1340; 1348 – 1350; 1356 – 1358; 1372 – 1374; 1388 – 1390; 1404 – 1406; 1414 – 1416; 1432 – 1434; 1458 – 1460; 1470 - 1472
R-3	10	0	0	1314 – 1316; 1328 – 1330; 1334 – 1336; 1348 – 1350 1362 – 1364; 1374 – 1376; 1388 – 1390; 1394 – 1396 1400 – 1402; 1442 – 1444
R-4	10	0	0	1348 – 1350; 1362 – 1364; 1374 – 1376; 1402 – 1404 1410 – 1412; 1420 – 1422; 1438 – 1440; 1444 – 1446 1456 – 1458; 1494 – 1496
R-5	13	0	0	1344 – 1346; 1348 – 1350; 1368 – 1370; 1374 – 1376 1384 – 1386; 1400 – 1402; 1402 – 1404; 1408 – 1410 1428 – 1430; 1438 – 1440; 1444 – 1446; 1490 – 1492 1492 – 1494
Totals	**57**	**0**	**0**	

For petrophysical analysis and core interpretation, well data such as wireline logging, core analysis data (RCAL and SCAL reports), mudlogging and PVT analysis from 6 (six) wells were utilized. The complete lists of well data are shown in Table 2.

The textural parameters (a-tortuosity constant, m-cementation factor, and n-saturation exponent) for petrophysical evaluation were taken from special core analysis (SCAL). The result obtained from SCAL analysis are shown in Table 3.

Formation water salinity for petrophysical evaluation was measured from PVT-Ten Ion water analysis. The Rw from the measurement is 0.34 ohmm at 75°F (~16.6 k ppm NaCl).

Standard deterministic petrophysical evaluation was carried out in this study. First, QC and environment correction for all the wireline log were performed. Second, petrophysical parameters such as Vsh, Phi, and Sw, were calculated from the wireline logs. Third, cutoff Vsh, PHIE, and Sw were applied to define net sand, net reservoir and net pay. Finally, all the calculated petrophysical parameters were calibrated with the core data, and the estimated net pay zone was validated with perforation zone.

***Table 2**. Well data availability of Ridho field*

Well	LAS	CALI	GR	SP	LLD	MSFL	RD	RMLL	RS	RHOB	ZDNC	NPHI	CNCF	DT	PEF	JPEG
R-1	✓	✓	✓	✓	✓	✓				✓		✓		✓	✓	✓
R-2	✓	✓	✓	✓			✓	✓	✓		✓		✓	✓	✓	✓
R-3	✓	✓	✓				✓	✓	✓		✓		✓	✓	✓	
R-4	✓	✓	✓	✓			✓	✓	✓		✓		✓	✓	✓	✓
R-5	✓	✓	✓	✓			✓	✓	✓		✓		✓	✓	✓	✓
R-6	✓	✓	✓	✓	✓	✓				✓		✓		✓	✓	✓

Well	Cutting	Mudlog/ Composite Log	Well Report	RCAL	SCAL	SWC	Geochem	PVT Ten Ion	Status
R-1	✓	✓	✓	✓	✓	✓			Oil Producer
R-2	✓	✓	✓	✓			✓	✓	Oil Producer
R-3	✓	✓	✓				✓	✓	Oil Producer
R-4	✓	✓	✓	✓			✓	✓	Injector
R-5	✓	✓	✓	✓			✓	✓	Oil Producer
R-6	✓	✓	✓	✓	✓	✓			Injector

***Table 3**. SCAL analysis for a, m, and n factor.*

Well	a	m	n	No. of Samples	#Sample No. - Depth (mMD)
R-2	1	1.98	1.8864	3	#4 (1389.9) #11 (1392.92) #25 (1397.35)
R-3	1	1.98	1.8685	3	#1 (1403.15) #18 (1409.11) #27 (1410.86)
R-4	1	1.98	1.8730	3	#5 (1401.06) #8 (1401.9) #17 (1404.12)

Core interpretation was done by plotting the core image in their corresponding depth and by logging and describing all the sedimentary structures, a change in grain size, and by identifying parasequence to create the geological interpretation. It is critical to validate the core depth if any misfit occurred. This was done by comparing depth of the core's Gamma vs the wireline's Gamma Ray curves. Beside the geological structures, other RCAL measurements such as porosity, permeability, and lithology description were used as supporting data to build geological interpretation.

RESULT

POD Sand to Sand Correlation Overview

Based on POD report of the Ridho Field, the sand units of Talang Akar and Lemat Formations were subdivided into three sand bodies including TAF SS-1, TAF SS-2, and Lemat-SS. The top and bottom of each sand units were defined based on the characters of the conventional wireline logs that encompasses GR, Resistivity, and Density-Neutron from R-1 and R-6 wells. Figure 3 exhibits the lithostratigraphy sand to sand correlation of R-1 and R-6 wells.

Table 4 shows the thickness of each sand body. As shown in Table 4, Sand TAF SS-2 is thickening to R-6 well while other sands seem to have quite consistent thickness between the two wells. Based on Figure 3, it is quite clear that the division of sand body can still be fine-tuned especially on TAF SS-2 as some shale breaks may separate the TAF SS-2 sand into different individual sands.

As more wireline data are available from 5 (five) additional development wells, the sand to sand correlations are updated with reference to R-1 and R-6 correlation. There are some justifications made to change sand bodies definition. Two (2) new sand bodies, TAF A1 and TAF A2, are introduced as the upper most sand body in the TAF. While, TAF SS-2 is sub-divided into three separated sand bodies TAF SS-2, TAF SS-3, and TAF SS-4. Figure 4 depicts the updated well correlations. The total gross thickness of each sand is shown in Table 5.

The gross thickness of each sand is inconsistent from well to well. Another strange finding from these tops picking is the significant thickness change of Lemat SS in R-2 well compared to those in other wells. This inconsistency rises an uncertainty on the sand unit definition for further modeling.

Palynology Analysis Result

Palynological analyses generally provide main information such as age and depositional environment. These information were taken based on the organic material or macerals presence in a sample, which may comprise: (1) wood, leaf and associated plant debris, (2) spores and pollen derived from plants which inhabit the land or freshwater, (3) pollen derived from plants that can tolerate brackish water, including mangroves, (4) algal cysts derived from freshwater, brackish and marine environments, (5) other organic-walled organisms including certain foraminifera. The individual occurrences, associations and relative abundances of the major fossil groups of various types of palynomorphs provide indications of the various depositional regimes and any changes from one depositional regime to another.

Three age markers are recognized based on palynology analysis in which all the markers predominantly correspond to Late Oligocene with very minor Early Miocene spores. These three time markers represent FDO (First Downhole Occurrence) of the fossil spores *Meyeripollis naharkotensis*, Peak or Acme of *Meyeripollis naharkotensis* and FDO of *Cicatricosisporites dorogensis*. The complete result of the pollen is shown in Table 6.

***Table 4**. Gross thickness of each sand body as defined in POD report of the Ridho field.*

Well	Sand Body	Top (mTVDSS)	Bottom (mTVDSS)	Gross Thickness
R-1	TAF SS-1	1311.35	1319.19	7.84
R-1	TAF SS-2	1327.72	1363.04	35.32
R-1	Lemat SS	1371.54	1403.56	32.02
R-6	TAF SS-1	1321.83	1329.62	7.79
R-6	TAF SS-2	1335.15	1375.55	40.4
R-6	Lemat SS	1382.95	1415.95	33

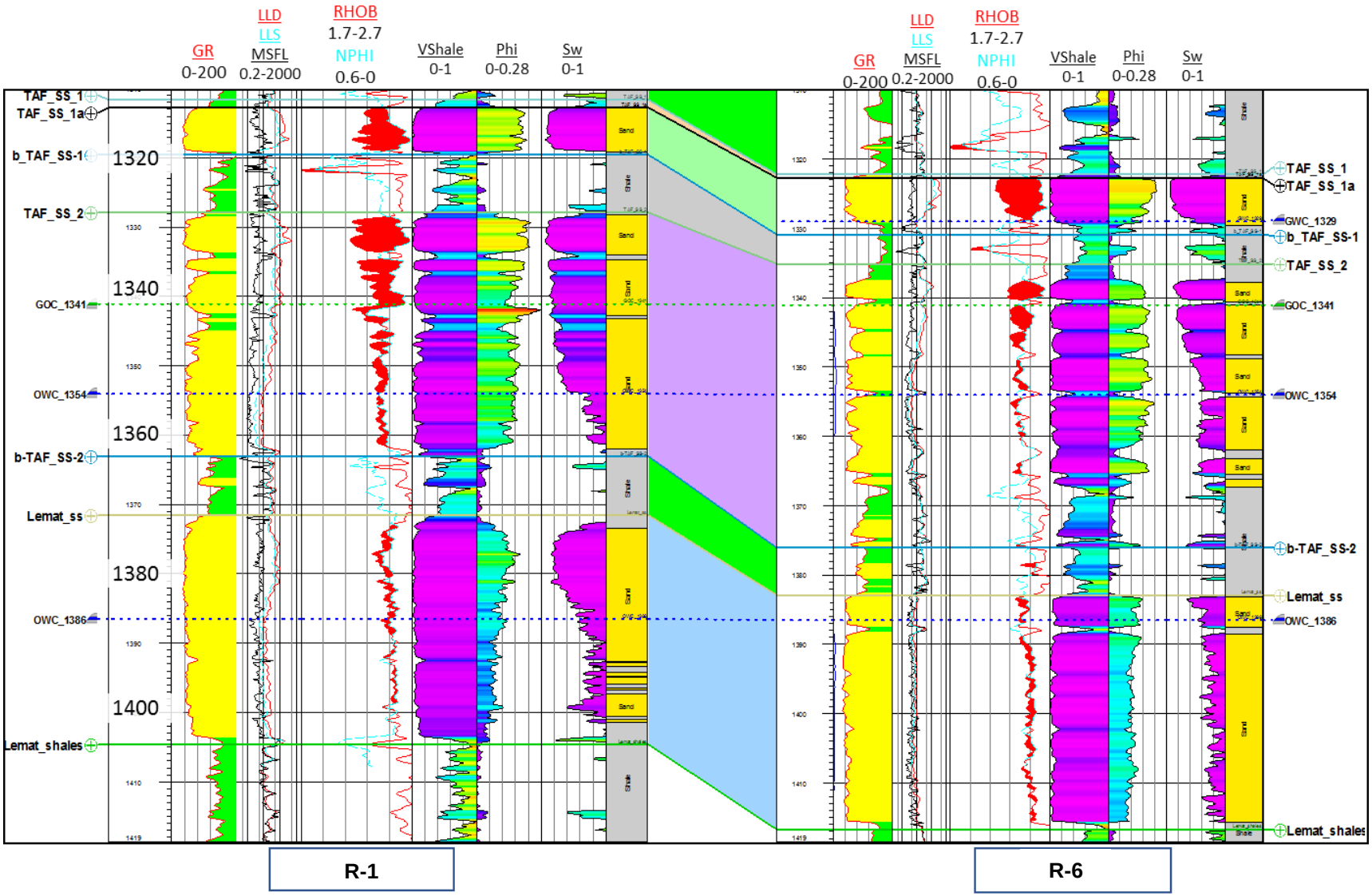


***Figure 3**: Lithostratigraphy correlation of R-1 and R-6 wells (plotted on TVDSS).*

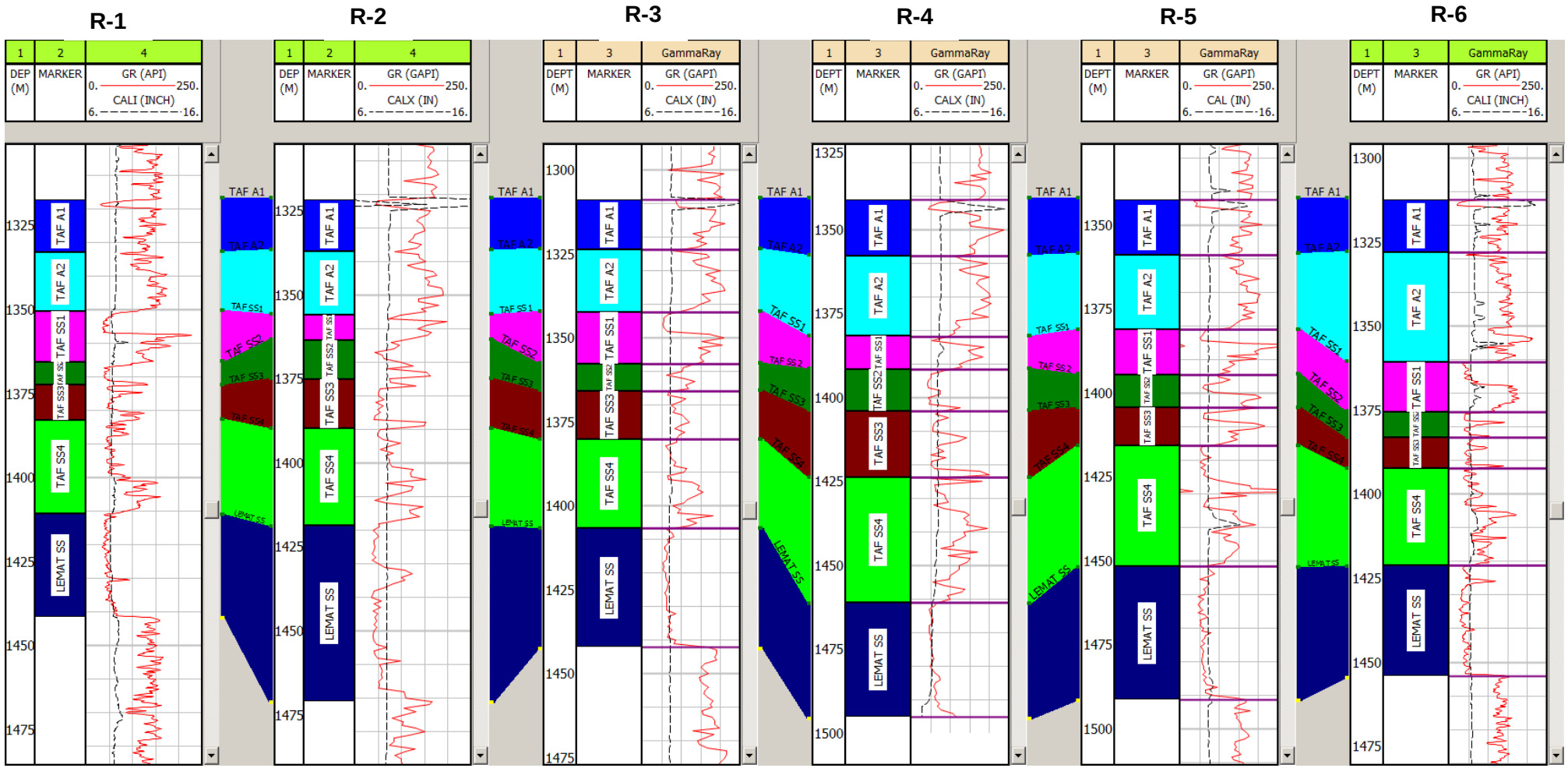


Figure 4: *Well correlation showing lithostratigraphy of the Ridho Field.*

***Table 5**. Gross thickness of TAF and Lemat SS based on Ridho wells.*

Well	Formation Tops (metres) (Gross Thickness)						
	TAF A-1	**TAF A-2**	**TAF SS-1**	**TAF SS-2**	**TAF SS-3**	**TAF SS-4**	**Lemat-SS**
R-1	1317.31 *(15.78)*	1333.09 *(17.46)*	1350.55 *(15.08)*	1365.63 *(6.88)*	1372.51 *(10.34)*	1382.85 *(28.04)*	1410.89 *(30.76)*
R-2	1321.68 *(15.27)*	1336.95 *(19.07)*	1356.02 *(7.42)*	1363.44 *(11.65)*	1375.09 *(14.72)*	1389.81 *(28.8)*	1418.69 *(52.28)*
R-3	1308.90 *(14.98)*	1323.88 *(18.52)*	1342.40 *(15.29)*	1357.69 *(8.15)*	1365.84 *(14.5)*	1380.34 *(26.32)*	1406.66 *(35.52)*
R-4	1341.14 *(16.84)*	1357.98 *(23.99)*	1381.79 *(9.61)*	1391.58 *(12.43)*	1404.01 *(19.85)*	1423.86 *(37.3)*	1461.16 *(33.97)*
R-5	1342.55 *(16.37)*	1358.92 *(22.36)*	1381.28 *(13.28)*	1394.56 *(9.89)*	1404.45 *(11.26)*	1415.71 *(35.96)*	1451.67 *(39.69)*
R-6	1312.35 *(15.73)*	1328.09 *(32.55)*	1360.63 *(14.82)*	1375.45 *(7.67)*	1383.12 *(9.26)*	1392.38 *(28.92)*	1421.30 *(32.80)*

***Table 6**. Age/zonation markers of Ridho field wells.*

Age/ Zonation	Comment	Well Name				
		R-1	**R-2**	**R-3**	**R-4**	**R-5**
?Early Miocene/ ?*F. trilobata*	This zone assigned based stratigraphic position above the FDO of *Meyeripollis naharkotensis* and *Cicatricosisporites dorogensis* and the presence of *F. trilobata.*	-	1326 (FSE) - 1340	-	-	-
Late Oligocene/ *M. naharkotensis*	The FDO of *Meyeripollis naharkotensis* at this interval may suggest the penetration of Oligocene age. This is supported by the presence of *Cicatricosisporites dorogensis.* The presence of *Proxapertites operculatus* at this interval interpret as reworked taxa from Eocene interval.	1320 (FSE) - 1358	1350 - 1358	1316 - 1444	1350 - 1496	1346 - 1494
	Peak *Meyeripollis naharkotensis*: This level recognized by the most abundant *M. naharkotensis.*	1360	1374	1364	1422	1386

***Table 7**. Chronostratigraphic unit definition in present study. (UTAF-Upper Talang Akar; LTAF-Lower Talang Akar; ULMF-Upper Lemat).*

Sand Unit	Top Marker	Bottom Marker	Well Top Depth (mMD)				
			R-1	R-2	R-3	R-4	R-5
UTAF-2	Coal Marker	FDO *Meyeripollis naharkotensis/ F.Trilobata*	1317	1321	1308.1	1341	1342.2
UTAF-1	FDO *Meyeripollis naharkotensis/*	Peak/Acme of *Meyeripollis naharkotensis*	1346	1348	1334.2	1364	1373.7
LTAF-2	Peak/Acme *Meyeripollis naharkotensis*	FDO *Cicatricosisporites dorogensis.*	1358	1372	1362	1422	1386
LTAF-1	FDO *Cicatricosisporites dorogensis.*	LDO *Cicatricosisporites dorogensis/* FDO *P.Kutchensis*	1380	1404	1388	1446	1437.6
ULMF-2	LDO *Cicatricosisporites dorogensis/* FDO *P.Kutchensis*	Bottom Lemat SS	1411	1436	1406.7	1461.2	1451.7

Based on the age marker from palynology analyis, new chronostratigraphic sand units were introduced. These new sand units are given in Table 7.

From the analyzed palynological slides, 90 palynomorphs species were identified. Twelve were fungal spore, 17 were pteridophytes and 47 were land angiosperm, 5 were mangrove plantation, 8 were back mangrove plantation and 1 was dinoflagellate cyst. The pollen facies interpretation example for R-1 is demonstrated in Figure 5. The complete palynofacies analysis for the other wells are presented in the appendices.

Petrophysical Analysis Result

The new top and bottom of the sand units replaced prior lithostratigraphy sand unit and were used in the subsequent petrophysical evaluation. The sand unit's NTG, Porosity, Vsh and Sw for each sand unit are shown by histogram in Figure 6. One can observe a relatively higher NTG in Lemat compared to that in the LTAF and UTAF. While from the Vsh and PHIE for reservoir layers, all the sand units can be categorized as a good-very good sand with maximum Vsh reservoir < 0.3, PHIE > 0.15. Unlike the NTG, the reservoir Vsh and PHIE show opposite trend where UTAF and LTAF possess better PHIE and Vsh. As R-4 is an injector well and structurally lower, the Sw of this well is the lowest compared to other wells, the vice versa can be seen in R-3.

The permeability are calculated by finding relationship between the core porosity and core permeability from RQI (Rock Quality Index) methods which is out of the scope of this publication. This method is used to generate the rock facies classifications.

The well section in Figure 8 exhibits petrophysical evaluation of the Ridho field wells (only producer wells are shown).

Core Interpretation

Figure 9 shows photograph of a core taken from a well that penetrated Lower Talang Akar Formation. Common features of the cores from this formation include:

- Pebbly sandstone at the base of parasequence, showing a lag deposit
- Common rock fragments indicating the sediment source is near
- Some ripple lamination, showing a traction current
- Cross bedded sandstone within transition from pebbly sandstone into organic shale
- Organic shale at the top of fining upward
- Common mud draped and flaser indicating a tidal process. Some mud drape is associated with cross bedding.

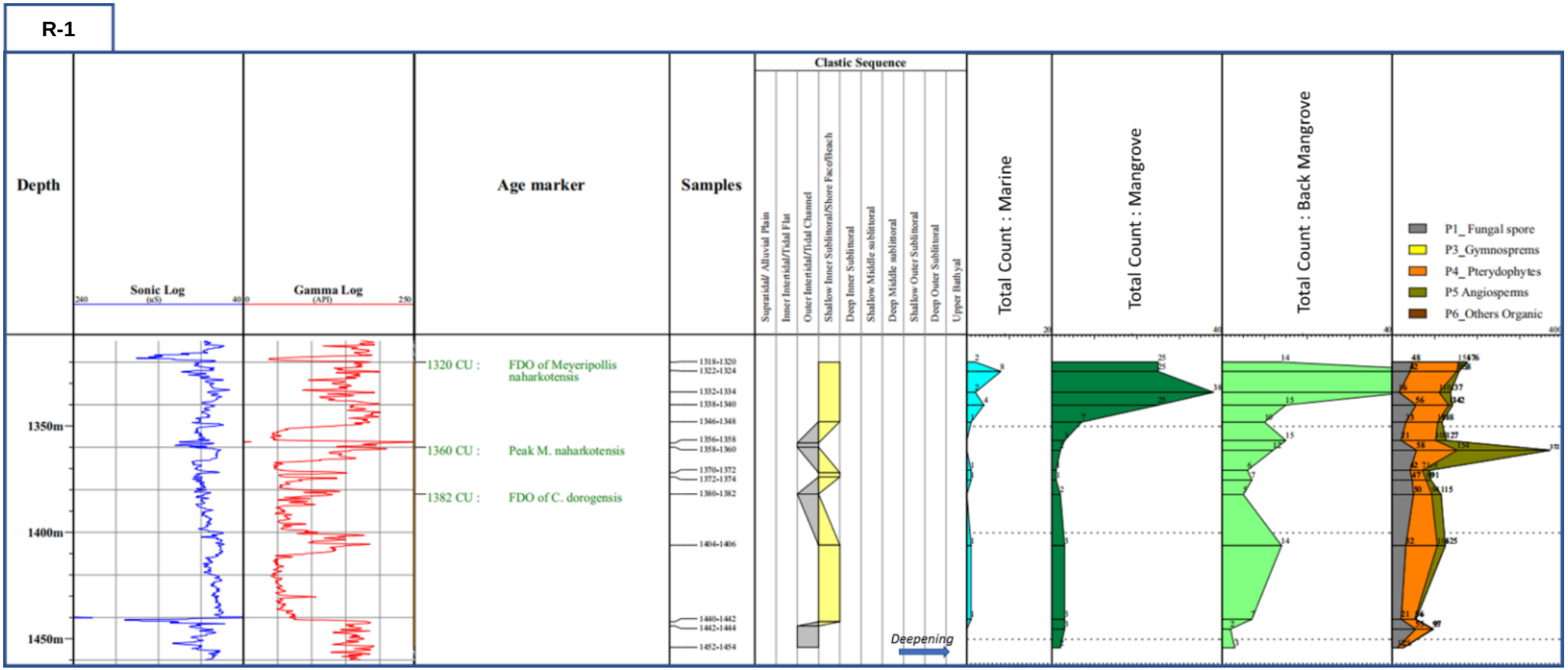


Figure 5: *Palynofacies analysis of R-1.*

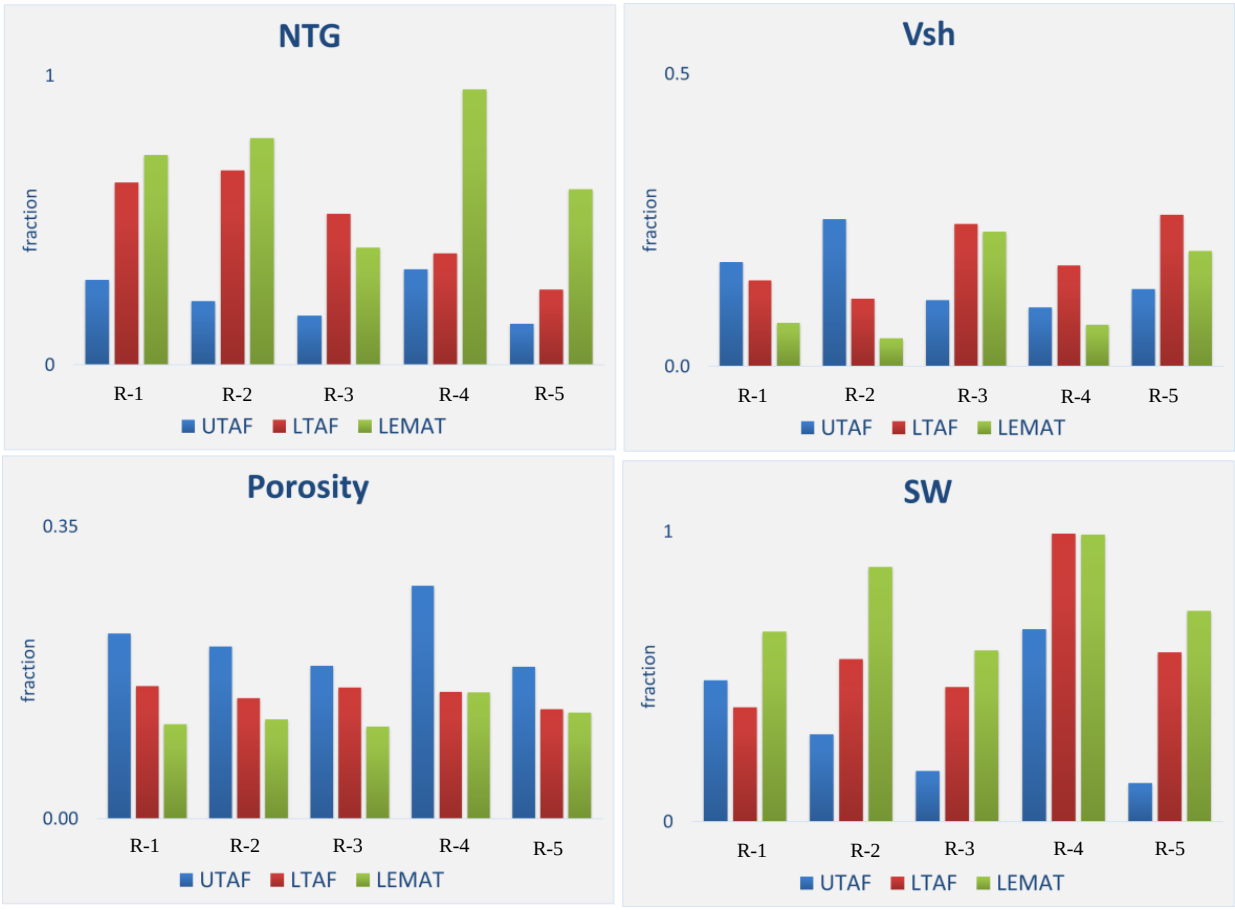


Figure 6: *Histogram shows the NTG, Vsh, Phie, and Sw of some wells in the Ridho field.*

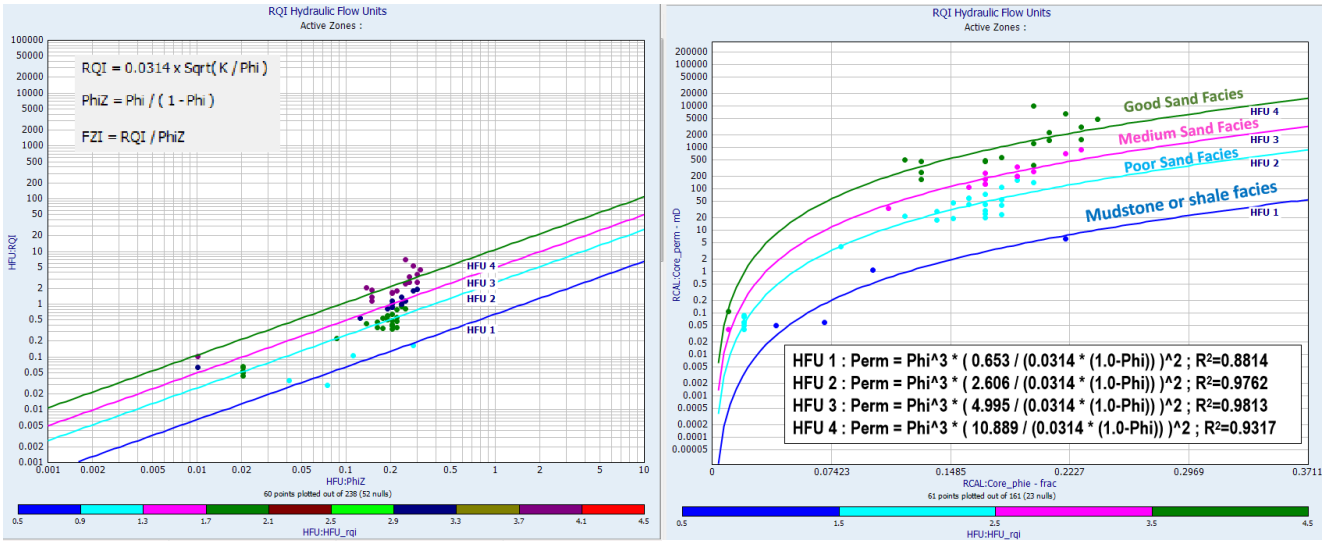


Figure 7: *(Left) The RQI vs PhiCore plot of R-2, R-3 and R-5. (Right) The HFU facies based on RQI methods.*

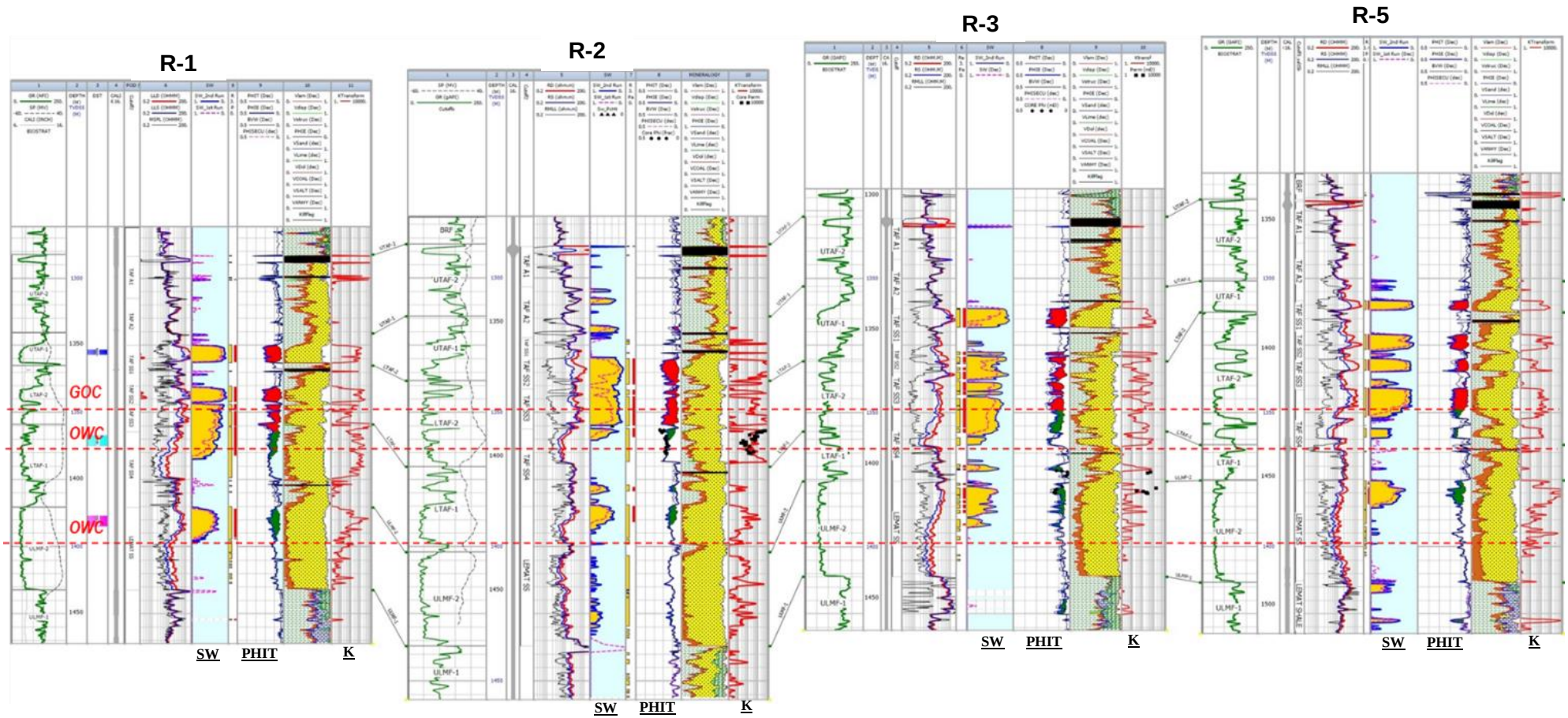


Figure 8: *Well section (flattened on TVDSS) of Ridho Field showing the result of petrophysical evaluation.*

The result from palynology analysis was also considered to interpret the depositional setting of Lower Talang Akar Formation. The palynology result is showing an intertidal with common back mangrove and higher plant spores. However, the mangrove and back-mangrove palynology signature is increasing to the Upper Talang Akar as the transgression occurred.

Common mud drape, flaser, lenticular sedimentary structures are showing traction current in tidal process. However, the depositional environment may not be too far from the source, as rock fragments are still remain. The Lower Talang Akar Formation is an early synrift sediment which common to have pebble of basement origin.

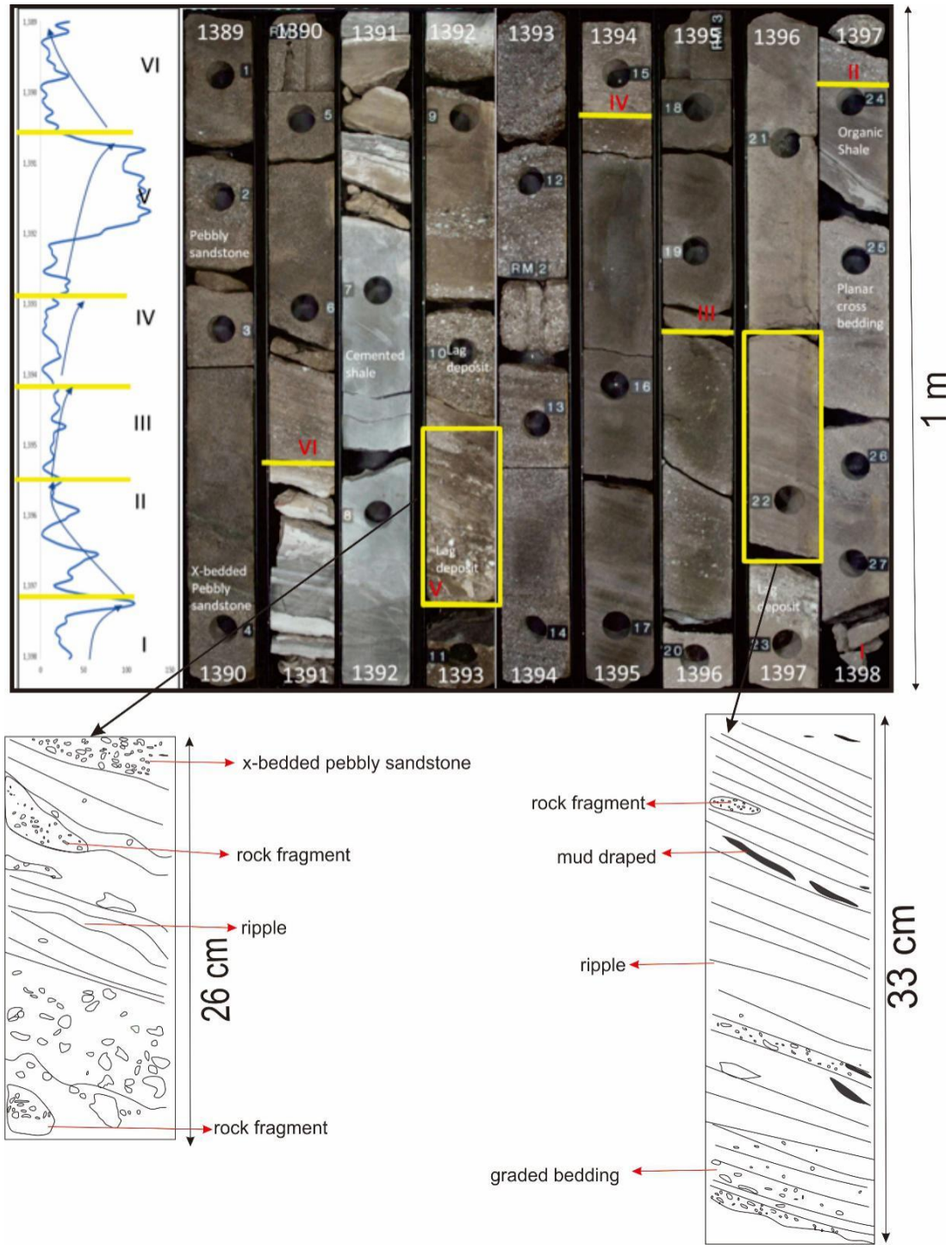


***Figure 9**: The core photograph along with core gamma with fining/coarsening upward signature of Lower Talang Akar Fm. The core gamma showing a good correlation to the grain size. The illustration below showing to emphasize of sedimentary structure in the core.*



Figure 10:

Typical of sandstone in the Upper Talang Akar Fm.

The core of Upper Talang Fm (left), is showing a cleaner sandstone with common cross bedding and mud drapes. As the marine transgression occurred, the sandstone become cleaner and rock fragment such as pebble become absent and the basement provenance is less prominent.

The reservoir geometry in this depositional environment is expected to be an isolated tidal channel which is perpendicular to the Oligocene shoreline.

DISCUSSION

A chronostratigraphy-driven well correlation was made for the Ridho Field, based on integration of data from wireline logs, petrophysical, palynology, sedimentology and special/routine core analyses. This integrated well correlation was not available when the field's POD was approved.

The palynology result is showing transgressive event from Lemat, Lower Talang Akar into the Upper Talang Akar Formation. The depositional environments changed from back-mangrove, mangrove, into shallow marine from Lemat, Lower Talang Akar, into Upper Talang Akar, respectively. As the transgression progressed, tidal influx become more persistent. This resulted in the development of isolated, sandy tidal channels within the upper part of Talang Akar, which should be perpendicular to Oligocene shoreline.

The transgression event created better reservoir quality due to the absence of mud and pebbles and better grain sorting within the Upper Talang Akar Formation. The better reservoir quality can be seen from core features, porosity-permeability data, and petrophysical analysis. The coarser grains associated with pebbles in the Lemat and Lower Talang Akar Formation indicate that their sediment source is relatively close, probably from exposed nearby basement. This was during a period of high energy fluvio-lacustrine depositional processes within the early synrift phase of North Palembang Sub-Basin development. However, the NTG of the Upper Talang Akar Formation is lower than Lower Talang Akar and Lemat Formation. This can be interpreted as the result of decreasing sediment supply and more distal environment that is also supported by a finer grains within the Upper Talang Akar Formation.

CONCLUSION

The chronostratigraphic sand units within Talang Akar and Lemat Formations in the Ridho Field were subdivided into: ULMF-2, LTAF-1, LTAF-2, UTAF-1, and UTAF-2. The depositional environments of Lemat and Lower Talang Akar Formation ranges from back-mangrove to mangrove, and then followed by shallow marine domination in the Upper Talang Akar Formation. The NTG in the Lemat and Lower Talang Akar is lower than it is in the Upper Talang Akar Formation. However, the reservoir property, such as Vsh, porosity, and permeability, are higher in the Upper Talang Akar than it is in the Lower Talang Akar and Lemat Formations.

REFERENCES

Barber, A.J., Crow, M.J., and Milsom, J.S. 2005. Sumatera: Geology, Resources and Tectonic Evolution. Geological Soeciety, London, Memoirs.

Bishop, M.G., 2001. South Sumatra Basin Province, Indonesia: The Lahat/Talang Akar-Cenozoic Total Petroleum System. USGS Open-file report 99-50S.

Cole, J. M., and Crittenden, S., 1997. Early Tertiary basin formation and the development of lacustrine and quasi-lacustrine/marine source rocks on the Sunda Shelf of SE Asia. In: Fraser, A. J., Matthews, S. J., and Murphy, R. W., eds., Petroleum Geology of Southeast Asia: Geological Society Special Publication No. 126, p. 147-183.

Courteney, S., Cockcroft, P., Lorentz, R., Miller, R., Ott, H.L., Prijosoesilo, P., Suhendan, A.R., Wight, A.W.R., 1990. South Sumatra. Indonesia - Oil

and Gas Fields Atlas, 3. Indonesian Petroleum Association, Jakarta, Indonesia.

De Coster, G. L. 1974. The geology of the Central and South Sumatra Basins. Proceedings of Indonesian Petroleum Association, 3rd Annual Convention, p. 77-110.

Hamilton, W., 1979. Tectonics of the Indonesian Region. Buletin Persatuan Geologi Malaysia (Bulletin Geological Society of Malaysia), 6, 1-345. Geological Society of Malaysia, Kuala Lumpur, Malaysia.

Longman, M.L., Siemers, C.T., Siwindono, T., 1992. Characteristics of low-relief carbonate mudbank reservoir rocks, Batu Raja Formation (Lower Miocene), Air Serdang and Mandala fields, South Sumatra Basin, Indonesia. In: Siemers, C.T., Longman, M.W., Park, R.K., Kaldi, J.G. (ed), Carbonate Rocks and Reservoirs of Indonesia: a Core Workshop, Indonesian Petroleum Association Core Workshop Notes, 1 (9).

Nichols, G. (2009). Sedimentology and stratigraphy (2nd ed.). Chichester, UK ; Hoboken, NJ: Wiley-Blackwell

Netherwood, R. 2000. The petroleum geology of Indonesia, overview of Indonesia's oil and gas industry. In: Indonesia 2000 Reservoir Optimization Conference, Jakarta, PT. Schlumberger Indonesia, p. 174-227.

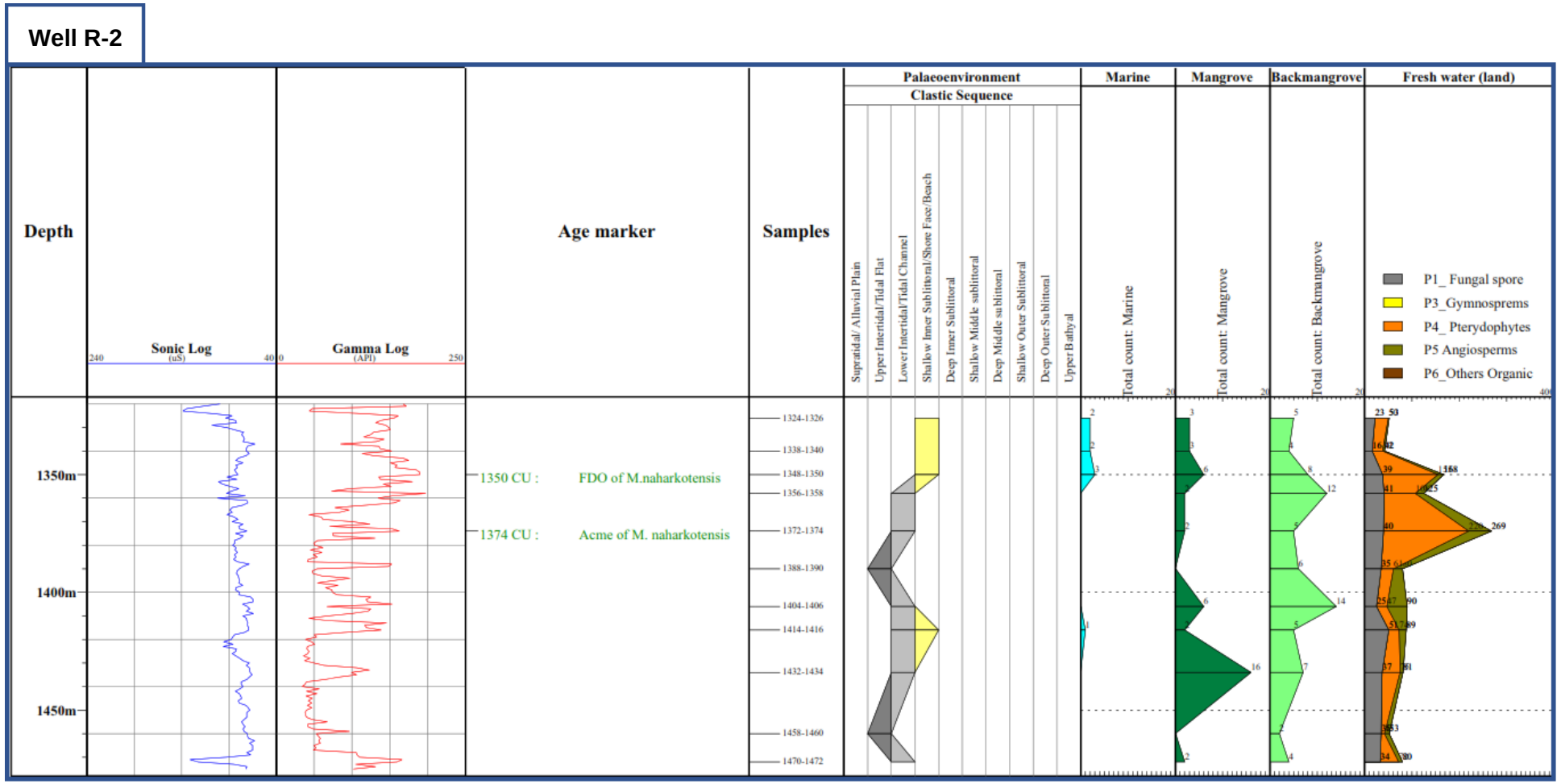
Situmeang, S.P., Zeliff, C.W., Lorentz, R.A., 1992. Characterisation of low relief carbonate banks, Baturaja Formation, Ramba A and B pools, South Sumatra, Indonesia. In: Siemers, C.T., Longman, M.W., Park, R.K., Kaldi, J.G. (ed), Carbonate Rocks and Reservoirs of Indonesia: a Core Workshop, Indonesian Petroleum Association Core Workshop Notes, 1 (8).

Suhendan, A. R., 1984. Middle Neogene depositional environments in Rambutan area, South Sumatra. Proceedings of Indonesian Petroleum Association, Thirteenth Annual Convention, May, 1984, p. 63-73.

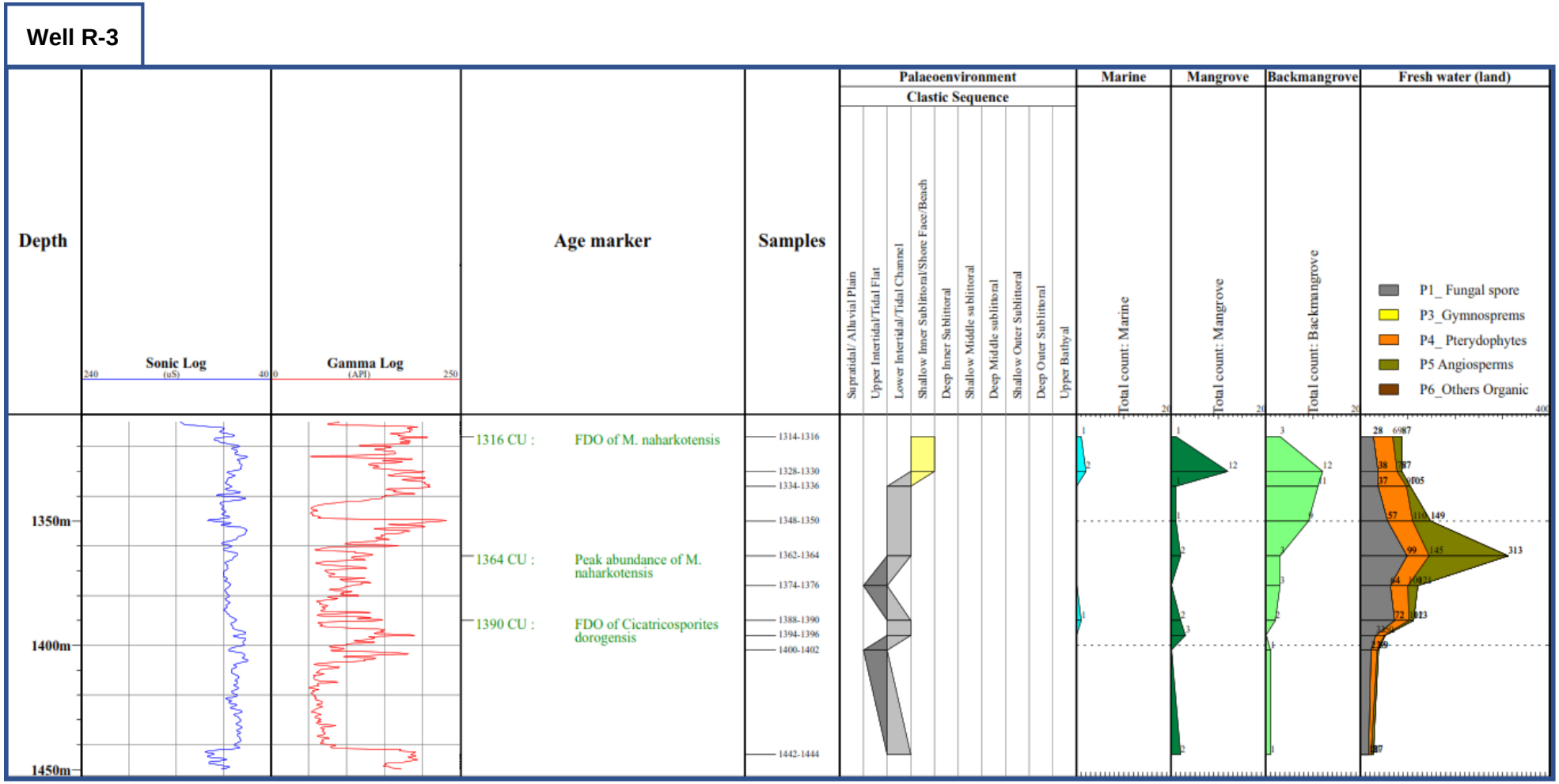
Syaifudin,M., Subroto, E.A., Noeradi,D., Kesumajana, A.H.P., 2015. Characterization and correlation study of source rocks and oils in Kuang area, South Sumatra basin: the potential of Lemat formation as hydrocarbon source rocks, Proceedings Indonesian Petroleum Association, Thirty-Ninth Annual Convention and Exhibition, Jakarta, Indonesia.

van der Zwan CJ. 1990. Palynostratigraphy and palynofacies reconstruction of the Upper Jurassic to Lowermost Cretaceous of the Draugen Field, offshore mid Norway. Rev Palaeobot Palyno. 62:157-186.

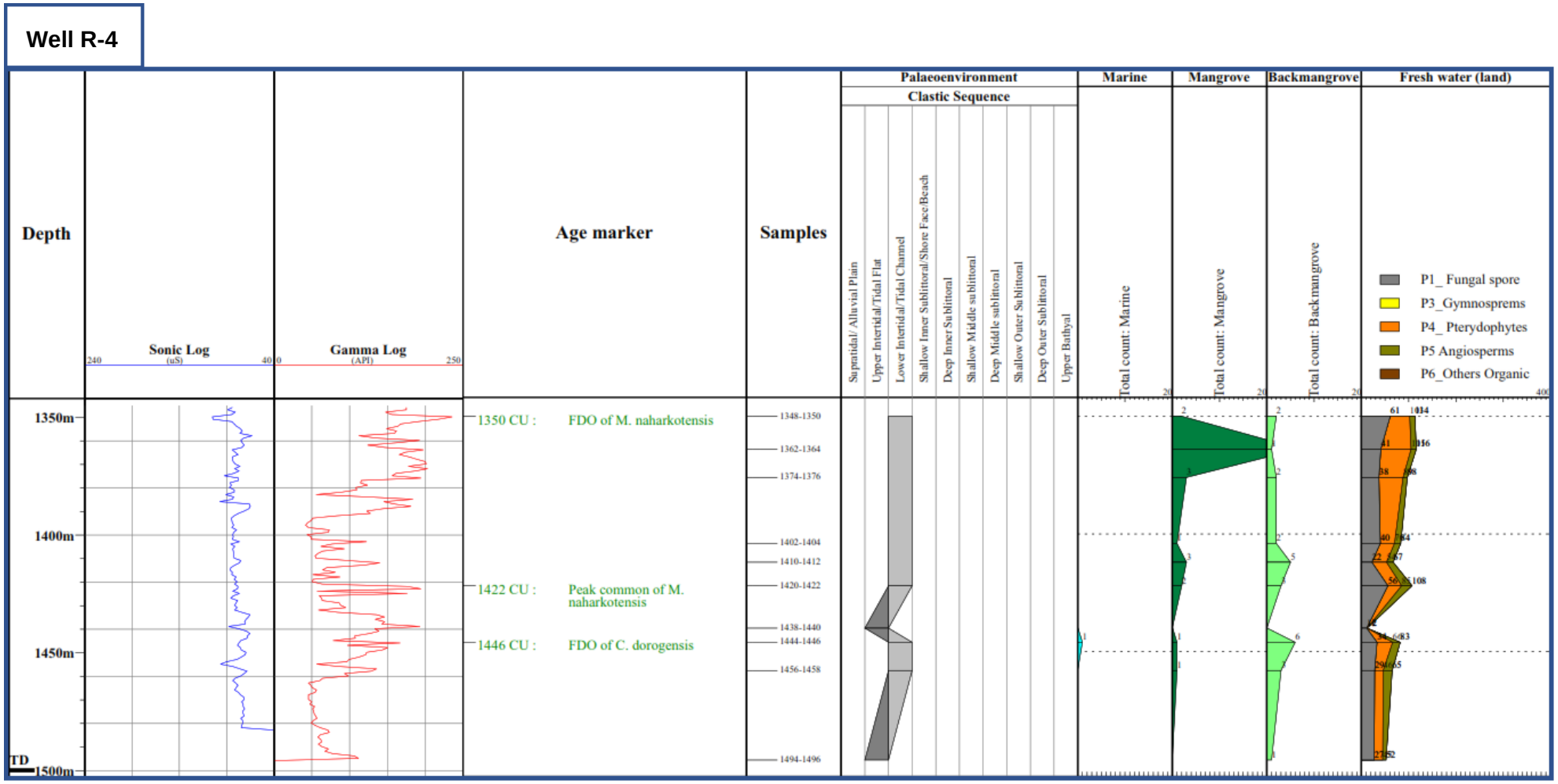
Whitaker MF, Giles MR, Cannon JC. 1992. Palynological review of the Brent Group, UK sector, North Sea. In: Morton AC, Haszeldine RS, Giles MR, Brown S, editors. Geology of the Brent Group. Geological Society of America Special Publications 61; p. 169-202.



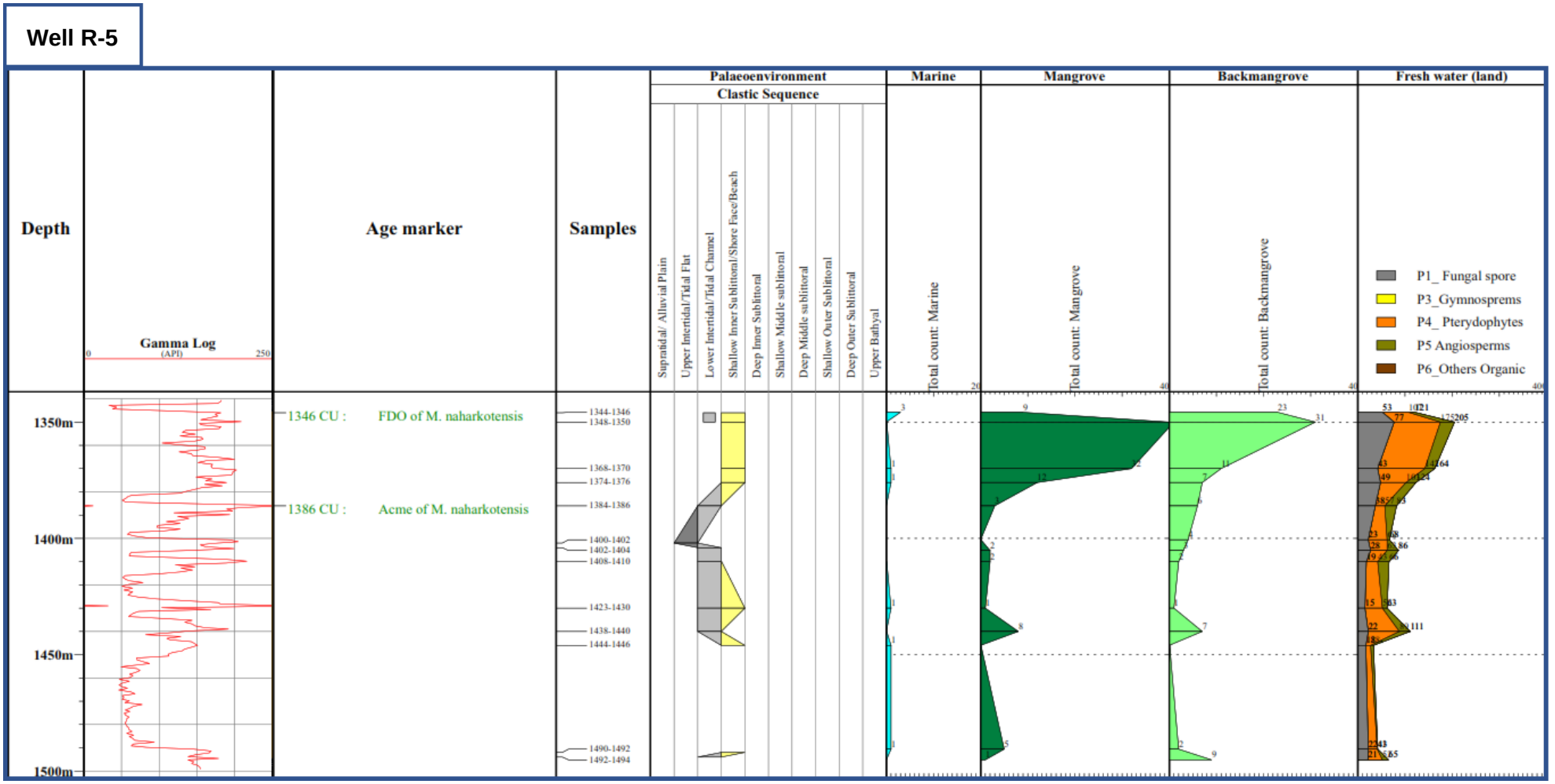
Appendix 1. *Palynofacies analysis of R-2*



Appendix 2. *Palynofacies analysis of R-3*



Appendix 3. *Palynofacies analysis of R-4*



Appendix 4. *Palynofacies analysis of R-5*